Scientia Marina 80(3)
September 2016, 409-421, Barcelona (Spain)
ISSN-L: 0214-8358
doi: http://dx.doi.org/10.3989/scimar.04370.15A

Three-dimensional connectivity during summer in the northern Gulf of California

Carolina Montaño-Cortés, Silvio G. Marinone

Departamento de Oceanografía Física, Centro de Investigación Científica y de Educación Superior de Ensenada (CICESE). Carretera Ensenada-Tijuana No. 3918, Zona Playitas, C.P. 22860, México. E-mail: marinone@cicese.mx

Summary: Connectivity studies in the Gulf of California are an important tool for improving the use and management of the gulf's natural resources. The goal of this work was to study the three-dimensional connectivity in the northern Gulf of California during two representative months of summer when most local marine species spawn. Passive particles were advected for eight weeks in a three-dimensional current field generated by a three-dimensional baroclinic numerical model. The results indicate that the locations of greatest particle retention were the Upper Gulf and the Seasonal Eddy. The Seasonal Eddy corresponded to the area of largest particle catchment because the continental coastal current carries most particles released in the Midriff Archipelago region; subsequently these particles were entrained in the seasonal cyclonic eddy, causing most of them to remain within it. We conclude that the continental coastal current and the Seasonal Eddy control the connectivity patterns in the northern Gulf of California.

Keywords: connectivity; northern Gulf of California; summer; HAMSOM; retention; continental coastal current; Seasonal Eddy.

Conectividad tridimensional durante el verano en el norte del Golfo de California

Resumen: Los estudios de conectividad en el Golfo de California (GC) son una herramienta importante para mejorar el uso y la gestión de los recursos naturales del golfo. El objetivo de este trabajo fue estudiar la conectividad tridimensional en el norte del Golfo de California (NGC) durante dos meses representativos de verano, ya que es la temporada con mayor desove de especies marinas. Se advectaron partículas pasivas durante ocho semanas en un campo de corrientes tridimensional generado por un modelo numérico baroclínico tridimensional. Los resultados indicaron que los lugares con mayor retención de las partículas fueron el Alto Golfo (UG) y el Remolino Estacional (SE). A su vez, SE fue el área de máxima captación de partículas debido a que la corriente costera continental transporta la mayoría de las partículas liberadas en las localidades ubicadas en la zona de las Grandes Islas, posteriormente estas partículas son atrapadas por el remolino ciclónico estacional lo que provocó que la mayoría de las partículas liberadas se queden dentro de éste. Por último, concluimos que la corriente costera continental y el remolino estacional controlan los patrones de conectividad en el NGC.

Palabras clave: conectividad; norte del Golfo de California; verano; HAMSOM; retención; corriente costera continental; remolino estacional.

Citation/Como citar este artículo: Montaño-Cortés C., Marinone S.G. 2016. Three-dimensional connectivity during summer in the northern Gulf of California. Sci. Mar. 80(3): 409-421. doi: http://dx.doi.org/10.3989/scimar.04370.15A

Editor: P. Puig.

Received: November 11, 2015. **Accepted**: May 13, 2016. **Published**: September 26, 2016.

INTRODUCTION

The northern Gulf of California (NGC) is one of the most productive marine regions in Mexico (Arvizu-Martinez 1987, Lluch-Cota 2007). This region displays high biodiversity (Ledesma-Vázquez and Carreño 2010) and three protected areas and two biosphere reserves have been established there to preserve marine species and benefit fishing (Marinone et al. 2008, Peguero-Icaza et al. 2011).

The circulation in the NGC has been described and explained from direct measurements of drifter buoys (Lavín et al. 1997), geostrophic currents from historical hydrographic data (Carrillo et al. 2002) and several current measurement observations. A conspicuous feature in this area is the presence of a seasonal reversible

gyre, which is cyclonic in summer (June to September) and anticyclonic in winter (November to April) with transitions in May and October (Beier and Ripa 1999, Lavín and Marinone 2003, Gutiérrez et al. 2004).

Knowing and understanding the circulation in any sea is important to understand its connectivity with surrounding areas. Connectivity studies are useful for the management of resources within that sea and also for understanding the dispersion patterns of tracers subjected to ocean hydrodynamics (Santiago-García et al. 2014).

Connectivity in the NGC has been characterized using numerical models. Marinone (2003) adapted the three-dimensional baroclinic numerical model HAMSOM to the Gulf of California, forcing it with tides, climatological winds and heat and fresh water fluxes at the sea surface and with climatological hydrography with the open boundary with the Pacific Ocean. From the results of the numerical model, several Lagrangian and connectivity studies have been done with different objectives. For example, Calderón-Aguilera et al. (2003) described the migratory patterns of blue shrimp related to the circulation in the northern gulf using the numerical model HAMSOM of Marinone (2003), explaining why postlarvae on the eastern side were larger (and older) than on the western side.

An important study of the coastal summer connectivity was that of Marinone et al. (2008), also using the same model currents. The results showed that the seasonal (low frequency) currents are more important than the tidal currents and the connectivity is basically downwind (following the cyclonic gyre). Marinone (2012) analysed the connectivity for the whole gulf using only surface currents and found that the largest retention from passive particles is at the northern gulf, where the gyre is present. However, these results are limited to descriptions of horizontal particle dispersion; i.e. the vertical positions of the particles have not been reported.

In a recent study, Santiago-García (2014) quantified the three-dimensional connectivity among 17 areas covering the entire gulf. The results are consistent with those cited above, but the three-dimensionality was reported vertically integrated. The vertical excursion of the particles has not been included in all these connectivity studies, though it has been reported as very large (Marinone 2006). Therefore, in this study, we extend the work of Santiago-García (2014) by continuing to track the vertical position of the particle trajectories and to quantify the connectivity relative to their position in the water column. For simplicity, we will focus on the summer season, which is when most local commercial species spawn (Marinone et al. 2008, Sánchez Velasco et al. 2012).

METHODOLOGY

Passive particles were allowed to be advected from an Eulerian velocity field obtained from the three-dimensional baroclinic HAMSOM model adapted for the Gulf of California by Marinone (2003, 2008). This model is based on a 0.83×0.83′ horizontal grid (approximately 1.3×1.5 km) and 12 vertical layers, whose lower limits are at depths of 10, 20, 30, 60, 100, 150, 200, 250, 350, 600, 1000 and 4000 m. Not all layers are present in each area: depending on the depth, the last layer in each position reaches the actual depth and is therefore variable. The model equations are momentum and continuity with fully prognostic temperature and salinity fields, which allow time-dependent baroclinic motions (Marinone 2003, Marinone et al. 2008). These equations are solved semi-implicitly (Marinone 2003, Marinone et al. 2008). The model was forced at the mouth of the gulf with climatologic fields of temperature and salinity and the primary tidal components (M_2, S_2, N_2, K_2, K_1, O_1, P_1, M_f, M_{sf}, M_m), and at the sea surface with clymatological wind field, and heat and fresh water (Marinone 2003, 2008, Santiago-García et al. 2014). The normal velocity to the coast is zero and the particles do not cross the solid coast.

The trajectories of the particles were calculated using an advection-related method involving an hourly Eulerian three-dimensional velocity field from the aforementioned model and a random walk contribution related to turbulent diffusion processes (Visser 1997, Proehl et al. 2005). The positions of the particles were obtained from the equations

$$X(t+\delta t) = X(t) + X_a(t) + R_x \sqrt{(6\, A_h\, \delta t\,)}, \quad (1)$$

$$Y(t+\delta t) = Y(t) + Y_a(t) + R_y \sqrt{(6\, A_h\, \delta t)}, \quad (2)$$

and

$$Z(t+\delta t) = Z(t) + Z_a(t) + R_z \sqrt{(6\, A_v\, \delta t)} + \delta t\, \partial A_v/\partial Z, \quad (3)$$

where X, Y and Z are the positions of particles in the zonal, meridional and vertical directions, particles obtained from inclusion of the velocity field V_a=(u, v, w) via the second-order Runge-Kutta method for the horizontal dimensions and using Euler for the vertical dimension (Marinone 2008, Santiago-García et al. 2014). The RK method was chosen as follows (Gutiérrez 2002): we constructed the velocity field from an analytical cyclonic gyre, compared the results obtained with the numerical integrations from Euler and 2nd- and 4th-order Runge methods with the analytical solution, and concluded that the 2nd-order Runge-Kutta method was enough. The particle speed at each position was obtained via bilinear interpolation of the instantaneous velocity fields in the numerical model. R_x, R_y and R_z are random variables varying between 1 and –1, with a mean value of zero and a standard deviation of 1/3. A_h and A_v are the horizontal and vertical turbulent diffusion coefficients from the numerical model, respectively. A_h is constant with a value of 100 $m^2\ s^{-1}$. A_v exhibits spatial and temporal variations and was obtained from the numerical model along with the velocity fields, with values ranging from 0 to 0.03 $m^2\ s^{-1}$. Equations (1) and (2) differ from (3) in one term, the last in (3), which takes into account the time and spatial variability of Av.

The model was validated with several studies. For example, the sea surface temperature of the gulf and the seasonal reversing gyre reported by Lavín et al. (1997)

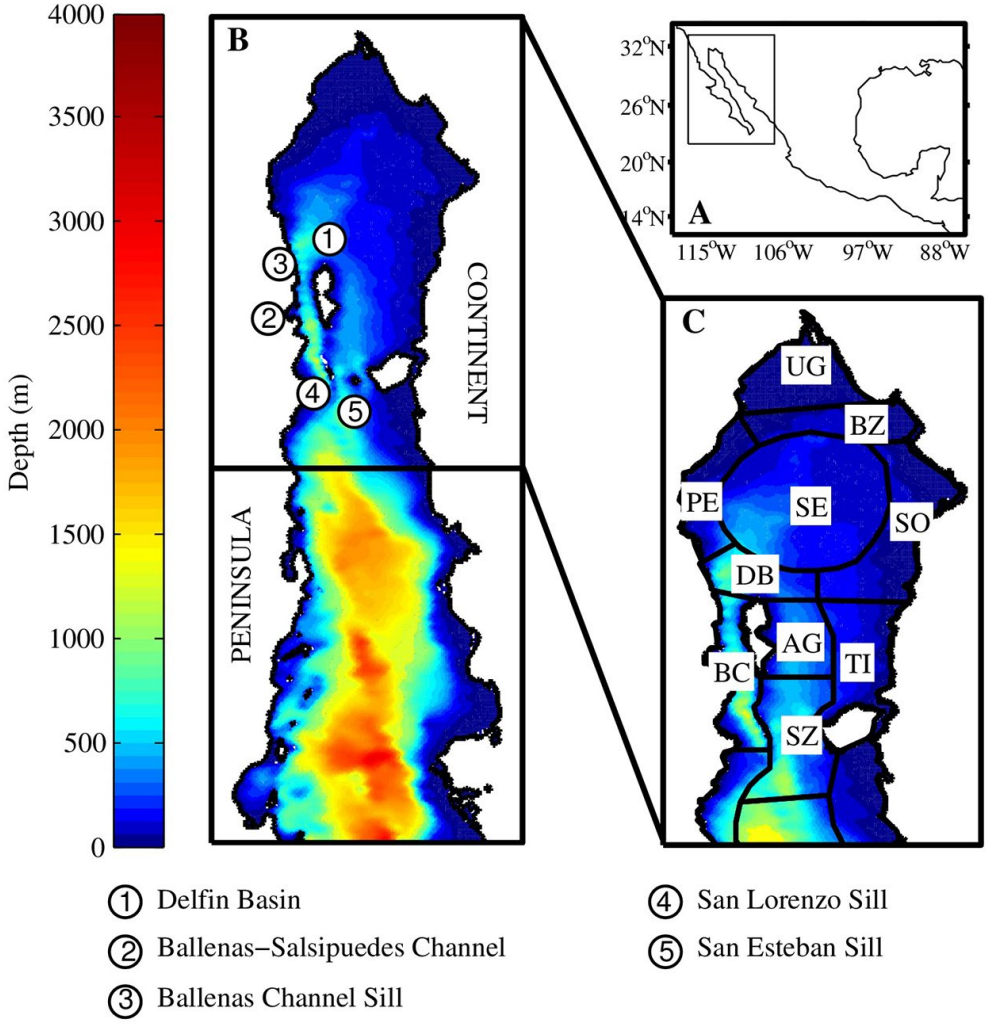

Fig. 1. – A, location of the Gulf of California. B, bathymetry of the Gulf of California with basins and sills that are part of the northern Gulf of California. C, study area and its division into ten provinces (Table 1).

was reproduced (Marinone 2003), as were the tides, sea surface and currents (Marinone and Lavín 2005), and the deep circulation around the large islands (Marinone 2008). Other studies related to larvae distribution and connectivity interpretations support a qualitatively good performance of the model (e.g. Cudney-Bueno et al. 2009, Munguia-Vega et al. 2014, Soria et al. 2013).

In this study of connectivity in the northern Gulf of California, passive particles were released on the first day of July in every layer of the model and in the ten regions shown in Figure 1 (Table 1). These regions are a subset of those defined by Santiago-García et al. (2014) for the entire gulf. They delimited the different areas based on the identification of trapping of transit zones using the Okubo Weiss parameter, the flow geometry and the general circulation of the gulf. The numbers of particles released were proportional to the area of the region (0.7 particles km^{-2}). At two, four, six, and eight weeks the final position of the particles was fixed and the number of particles within each region was counted and reported as a percentage. From this information, a connectivity matrix $C_{ij}(t)$ was constructed, in which the horizontal axis *i* represents the arrival area or final destination of the particles, the vertical axis *j* represents the areas where the particles were released, and *t* is the week when the positions of the particles released in July were observed. Note that the diagonal elements represent the particles that remain or return to the release areas. The depth of the particles of each element of C_{ij} was average and reported as $P_{ij}(t)$.

Table 1. – Areas of the northern Gulf of California (Santiago-García et al. 2014).

Acronyms	Name
UG	Upper Gulf
BZ	Buffer Zone
PE	Peninsular Eddies
SE	Seasonal Eddy
SO	The northern coast of Sonora
TI	North of the Tiburón Island
AG	East of the Ángel de la Guarda island
DB	Delfín Basin
BC	Ballenas-Salsipuedes Channel
SZ	Sills Zone

As can be deduced, this process results in many matrices (12 layers and 10 areas for 2, 4, 6, and 8 weeks) and in order to condense this information we constructed two types of matrice:

A retention matrix, R_{ij}. For each layer of release, the diagonal elements of C_{ij} were accommodated in each

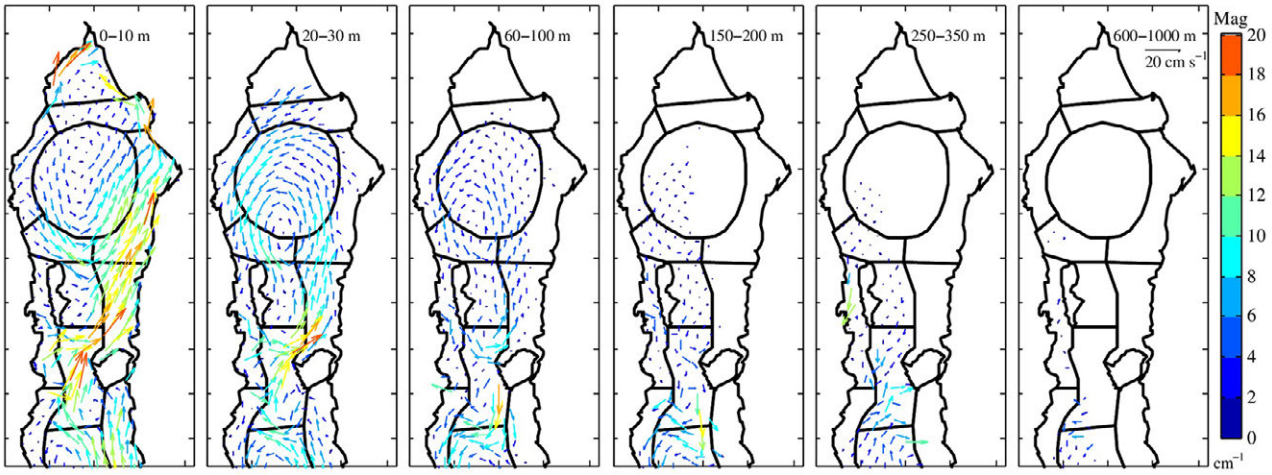

Fig. 2. – Average currents for the months of July and August for the indicated model layers.

row of R_{ij} and now the horizontal axis (i) represents the released area and the vertical axis (j) the model layer of release. It indicates the percentage of particles that remained in or returned to the area and depth from where they were released. In the same way the final average depth matrix was constructed.

A maximum catchment matrix. M_{ij}. From each row (i) of C_{ij}, excluding the diagonal, and for each layer (j) of release, the cell with the maximum percentage of particles exported are stored in M_{ij} with a digit indicating the area of arrival (see below in results). So this matrix indicates the region that caught the highest percentage of released particles from each layer of the NGC's areas. Also, the associated final average depth matrix was constructed.

Combined with the results of the connectivity and average depth matrices, we used maps showing the final geographic positions of the particles at various times as a colour code showing the depth of each particle. Similarly, we used histograms to show the percentages of connectivity of each region of the NGC in relation to the surrounding NGC.

RESULTS AND DISCUSSION

Circulation patterns

The typical circulation during July and August (Fig. 2) includes a wide, strong current (10-20 m s^{-1}) down to depths of as much as 30 m along the continental coast. Along the Baja California Peninsula, there is a narrow, strong current (6-20 m s^{-1}) flowing towards the Upper Gulf. The mentioned seasonal cyclonic eddy that is characteristic of the summer (Lavín et al. 1997, Beier and Ripa 1999, Carrillo et al. 2002) is present.

Retention matrix

Figure 3 shows the connectivity retention matrix and the associated average depth matrix 8 weeks after the particles were released. The vertical and horizontal axes correspond to the location and depth where the particles were released, respectively. The colours denote the percentages of particle retention and the mean

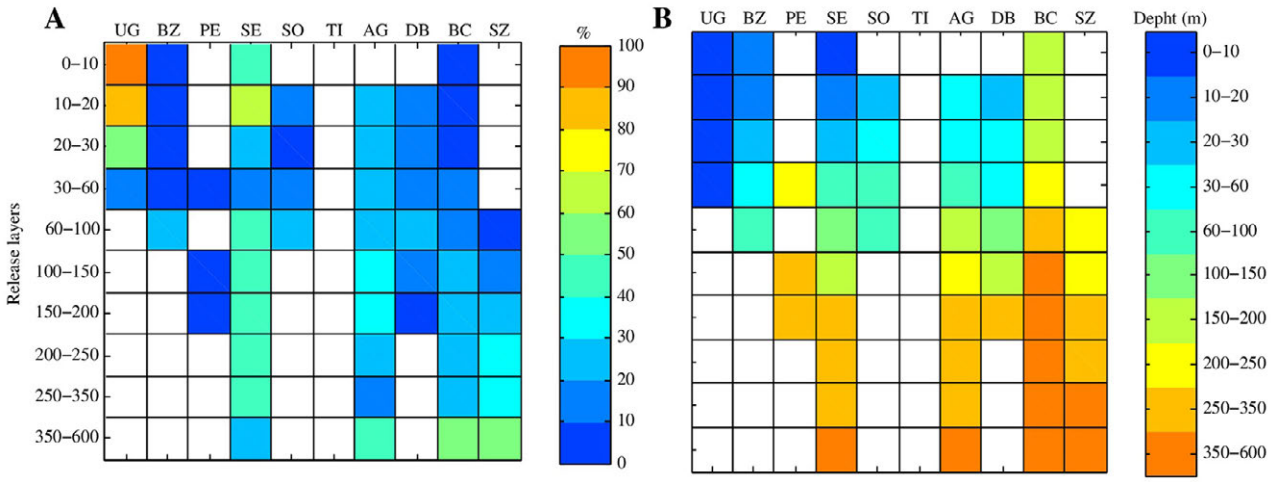

Fig. 3. – A, retention matrix, showing the percentage of particles located in the diagonal of connectivity matrices of each released layer, i.e. the percentage that ends in the same area after eight weeks. B, average depth matrix associated to the retention matrix, which shows the final average depth of the retained particles. The horizontal and vertical axes denote the area and layer of release, respectively. For clarity, cells with connectivity less than or equal to 5% are not coloured. Note that the final vertical position can be different from the released layer.

Table 2. – Four cases inferred from the retention matrix.

Case	Location	Description
Highest retention	Upper Gulf	Areas where the highest percentages of particles were retained in most layers where they were released.
	Seasonal Eddy	
Transition areas	North of Tiburón Island	Areas where high percentages of particles were carried from the areas of release to other areas.
	Peninsular Eddies	
	Sills Zone	
	Buffer Zone	
	Northern coast of Sonora	
Return areas	Delfín Basin	Areas where high percentages of particles left and returned to the area of release.
	East of the Ángel de la Guarda island	
High variability	Ballenas-Salsipuedes Channel	Area where retained particles were carried deeper than where they were released.

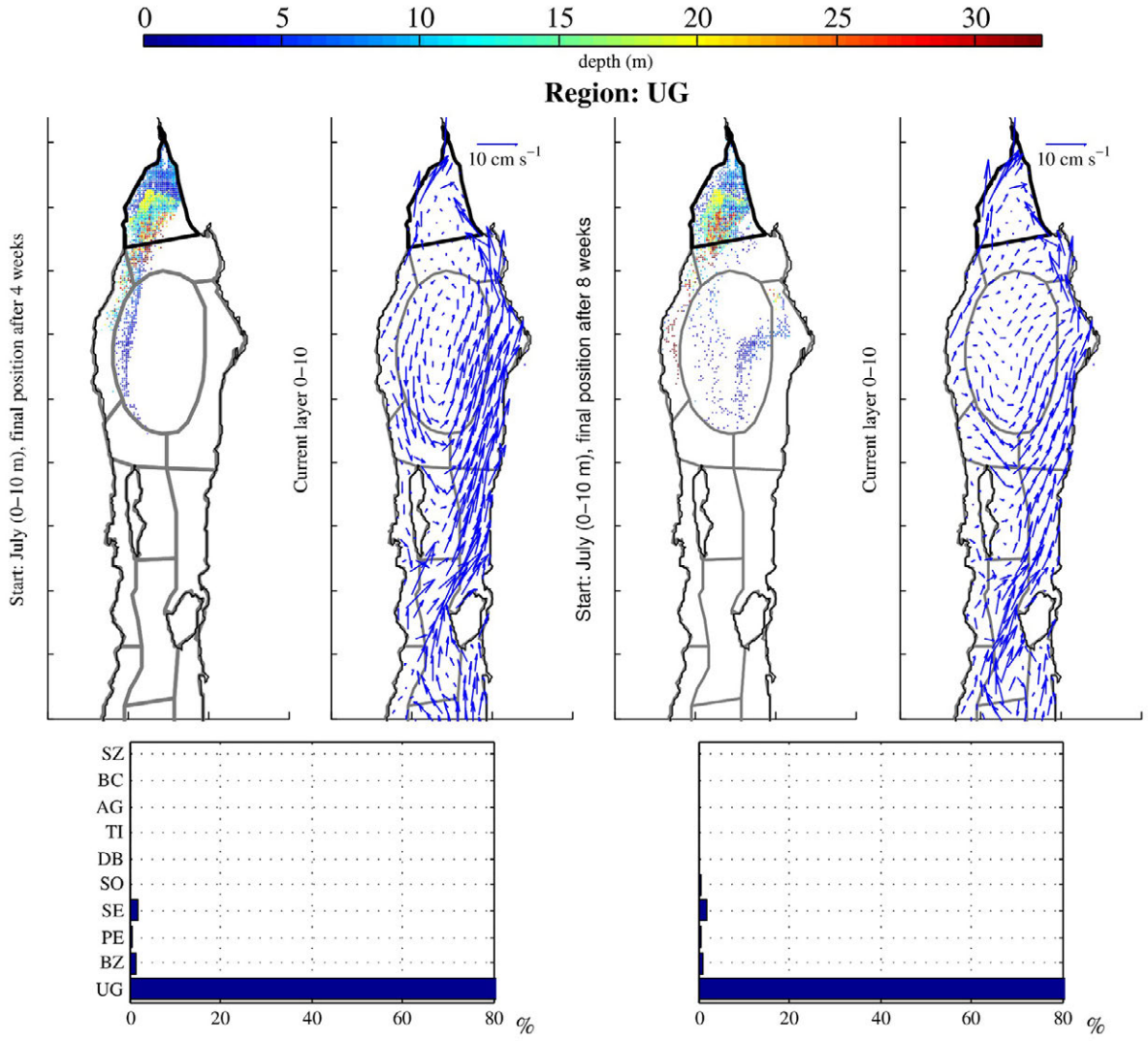

Fig. 4. – Map of final positions of particles released in the Upper Gulf's first layer, for the fourth and eighth week after the release of particles. The release area is shown in black and the other areas in grey polygon. The colour bar represents the depth at which each particle is located. The histogram shows the percentage of particles retained or transferred to other regions. Current maps correspond to the layer in which the percentage of particles retained is concentrated, in the fourth and eighth week after particle release.

depths of those particles. For example, the Ballenas-Salsipuedes Channel retained slightly more than 5% of the particles released in the uppermost layer (0-10 m) (Fig. 3A), and these particles were observed at depths of 150 to 200 m (Fig. 3B).

Based on Figure 3 and the dispersion pattern of the particles after eight weeks, four cases were observed (Table 2). These cases are described next.

Highest retention

The locations with the highest retention were the Upper Gulf and the Seasonal Eddy, as observed by Santiago-García et al. (2014). This retention is related to the fact that the coastal continental current prevents particles from leaving (Santiago-García et al. 2014) and to weaker currents and an anticyclonic gyre that traps

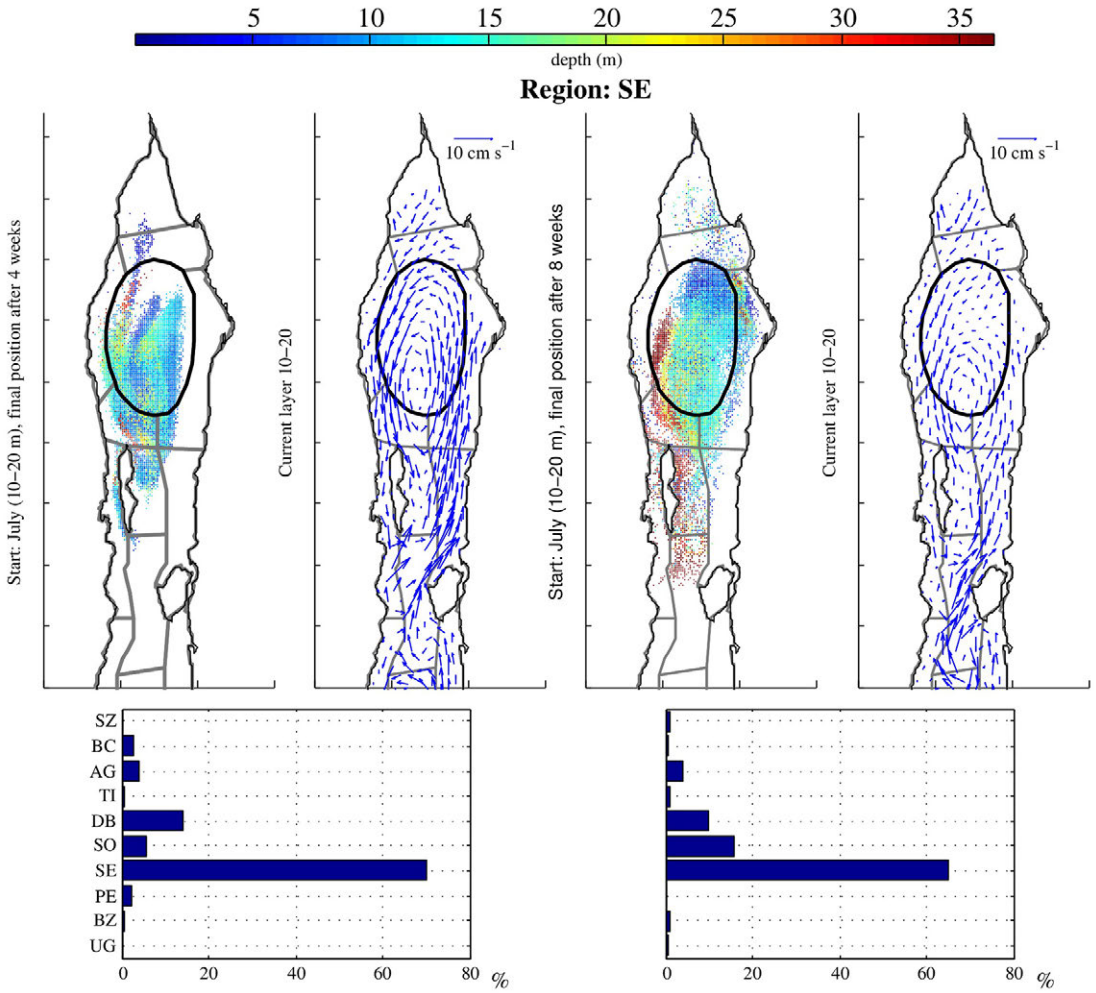

Fig. 5. – Map of final positions of particles released in the Seasonal Eddy's second layer, in the fourth and eighth week after the release of particles. The release area is shown in black and the other areas in grey polygon. The colour bar represents the depth at which each particle is located. The histogram shows the percentage of particles retained or transferred to other regions. Current maps correspond to the layer in which the percentage of particles retained is concentrated, in the fourth and eighth week after particle release.

particles for more than a month (Fig. 4) (Marinone et al. 2011, Marinone 2012). In the Upper Gulf we found that this retention changes with depth (Fig. 3A), in some cases particles remain at the same depth and in other they change position in the water column; this excursion was not observed in the work of Santiago-García et al. (2014) as the data were vertically averaged.

The Seasonal Eddy region also displayed a high percentage of retention for the most layers: more than 40% of the particles released in this area (Fig. 3A). This retention is related to the seasonal cyclonic eddy extending across most of the NGC region (Fig. 5) and nearly throughout the water column (Fig. 2), which causes trapping of particles in this area for as long as two months (Velasco Fuentes and Marinone 1999, Gutiérrez et al. 2004). It can be observed that particles released in the upper 30 m remain in the same model layer (Fig. 3B); the rest of the water column shows less vertical excursion.

Transition areas

The transition areas are those with low percentages of particle retention due to greater particle dispersion towards other areas.

The least particle retention was observed at the north of the Tiburón Island region, where there were no significant percentages of retained particles in most layers (all percentages were less than 5%) (Fig. 3A). This pattern was strongly controlled by the continental coastal current flowing towards the NGC throughout the water column (Fig. 6) and by an increase in current velocity caused by the presence of narrow channels and the restriction in the area due to the Great Islands (Gutiérrez et al. 2004, Peguero-Icaza et al. 2011).

Subsequently, this current flowed towards the Tiburón Island region and along the northern coast of the Sonora region and, as a result, most particles were carried outside this area, so the percentages of particle retention were below 15% in most layers (Fig. 3A). The particles that remained in the Sonora region were concentrated at greater depths (Figs 7 and 3A). Downstream, the continental coastal current interacted with the seasonal cyclonic eddy, and the particles released from the interior of the eddy were carried to neighboring regions (Fig. 7).

A gradual increase in particle retention with increasing depth was observed in the Sills Zone (Fig. 3). A dominant northward current explains this behaviour,

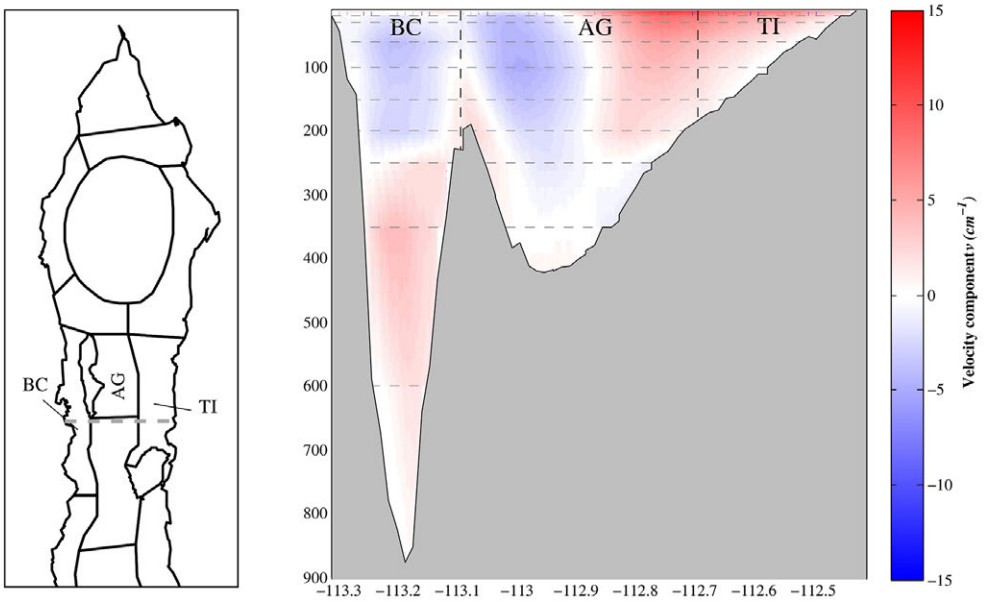

Fig. 6. – Vertical section between the Midriff Archipelago area (grey dashed line). The colour bar represents the normal current direction north (red) and south (blue). The grey horizontal dashed lines are the model's layers.

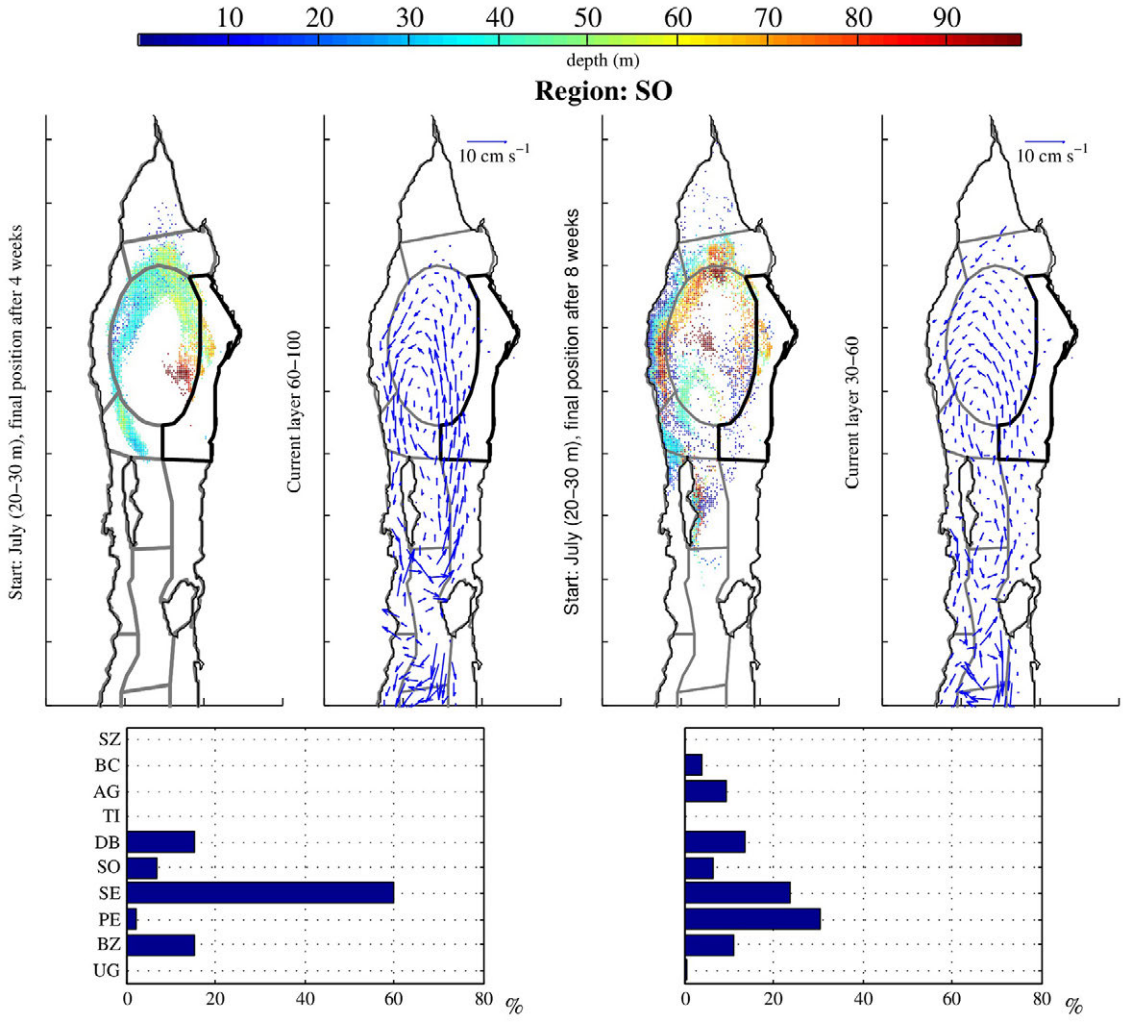

Fig. 7. – Map of final positions of particles released in the northern coast of Sonora's second layer, in the fourth and eighth week after the release of particles. The release area is shown in black and the other areas in grey polygon. The colour bar represents the depth at which each particle is located. The histogram shows the percentage of particles retained or transferred to other regions. Current maps correspond to the layer in which the percentage of particles retained is concentrated, in the fourth and eighth week after particle release.

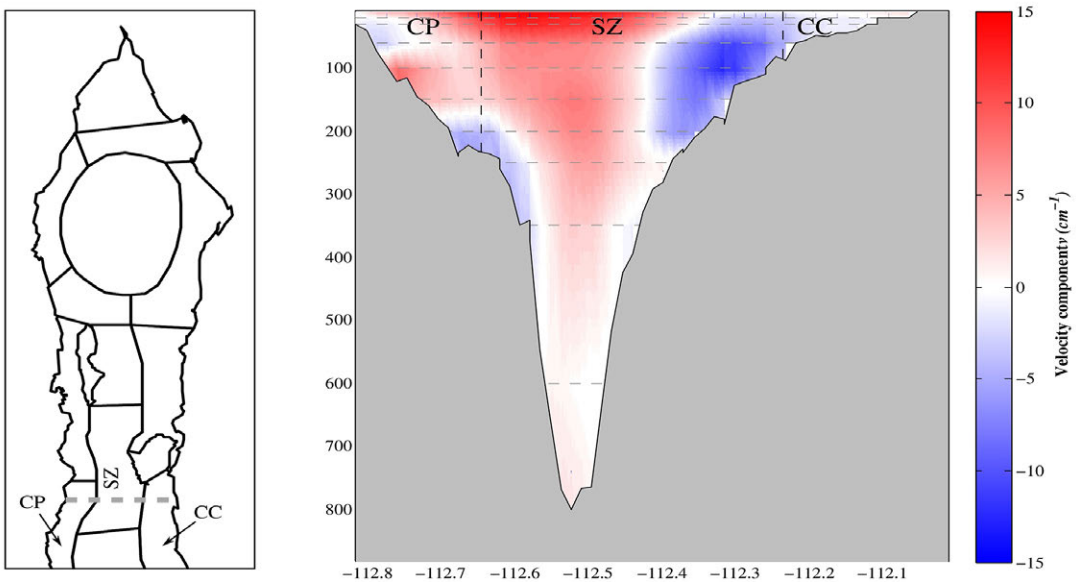

Fig. 8. – Vertical section of the Sills Zone (grey dashed line). The colour bar represents the normal current direction: north (red) and south (blue). The grey horizontal dashed lines are the model's layers.

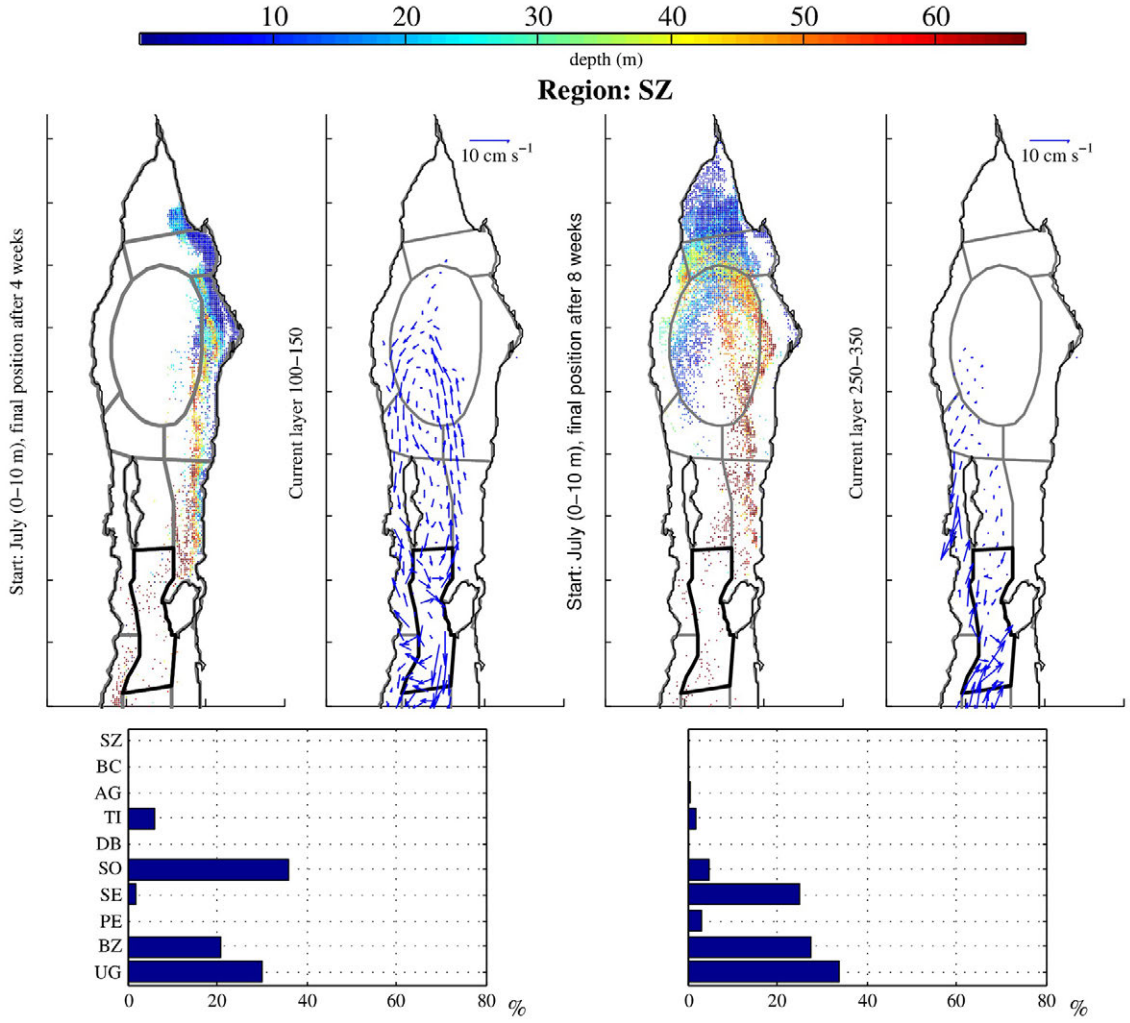

Fig. 9. – Map of final position of particles released in the Sills Zone's first layer, in the fourth and eighth week after the release of particles. The release area is shown in black and the other areas in grey polygon. The colour bar represents the depth at which each particle is located. The histogram shows the percentage of particles retained or transferred to other regions. Current maps correspond to the layer in which the percentage of particles retained is concentrated, in the fourth and eighth week after particle release.

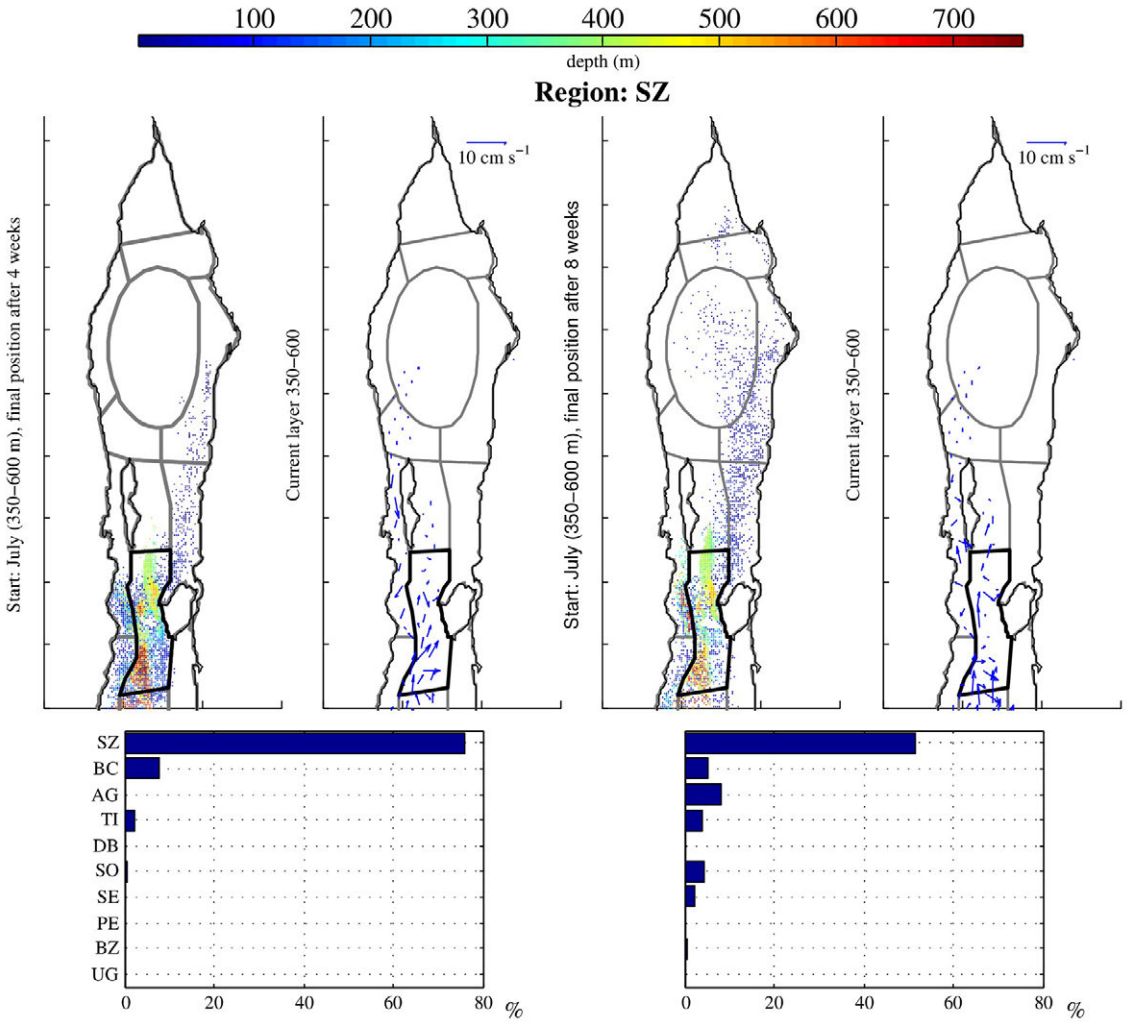

Fig. 10. – Map of final position of particles released in the Sills Zone's tenth layer, in the fourth and eighth week after the release of particles. The release area is shown in black and the other areas in grey polygon. The colour bar represents the depth at which each particle is located. The histogram shows the percentage of particles retained or transferred to other regions. Current maps correspond to the layer in which the percentage of particles retained is concentrated, in the fourth and eighth week after particle release.

with velocities decreasing along the vertical axis (Fig. 8). This pattern can be observed more clearly at the particle destinations (Figs 9 and 10). At the surface layer, retention is minimum and the particles are exported to the northern area (Fig. 9). From 60 m the percentage of retention increases (Fig. 3A). Figure 10 clearly shows the position of particles with a ~60% retention, with depth averages of 350-600 m, though some particles remain at depths of less than 300 m. On the other hand, some particles leave the Sills Zone to the south of the Gulf of California (Fig. 10).

Return areas

The return areas are east of Ángel de la Guarda island and Delfín Basin. These areas are locations where the particles were released, left the area and returned after a certain period of time. In the Ángel de la Guarda area, the released particles were carried towards the interior of the gulf by the continental coastal current until they met the cyclonic eddy during the fourth week. This eddy carried the particles back to where they were released after eight weeks (Fig. 11). In the Delfín Basin, the particles were carried towards the current leading to the Ballenas-Salsipuedes Channel and towards the southern gulf. However, after passing Ángel de la Guarda island, most of these particles were carried by the current leading to the interior of the gulf (Fig. 12) and returned to the Ballenas-Salsipuedes Channel.

High variability

Particle retention in the Ballenas-Salsipuedes Channel region gradually increased with depth (from ~5% to ~60%, Fig. 3A). The retained particles were located in deeper areas than where they were released (Fig. 3B). This behaviour is explained by the strong vertical circulation and mixing of this region, where gravity currents in northern and southern sills of the Ballenas-Salsipuedes Channel, which flow southward and northward, respectively, have been reported (López et al. 2006, 2008) and reproduced with the numerical model used here (Marinone 2008). These currents meet at depth, causing convergences in lower zones and divergences in upper zones in the channel (Marinone 2008).

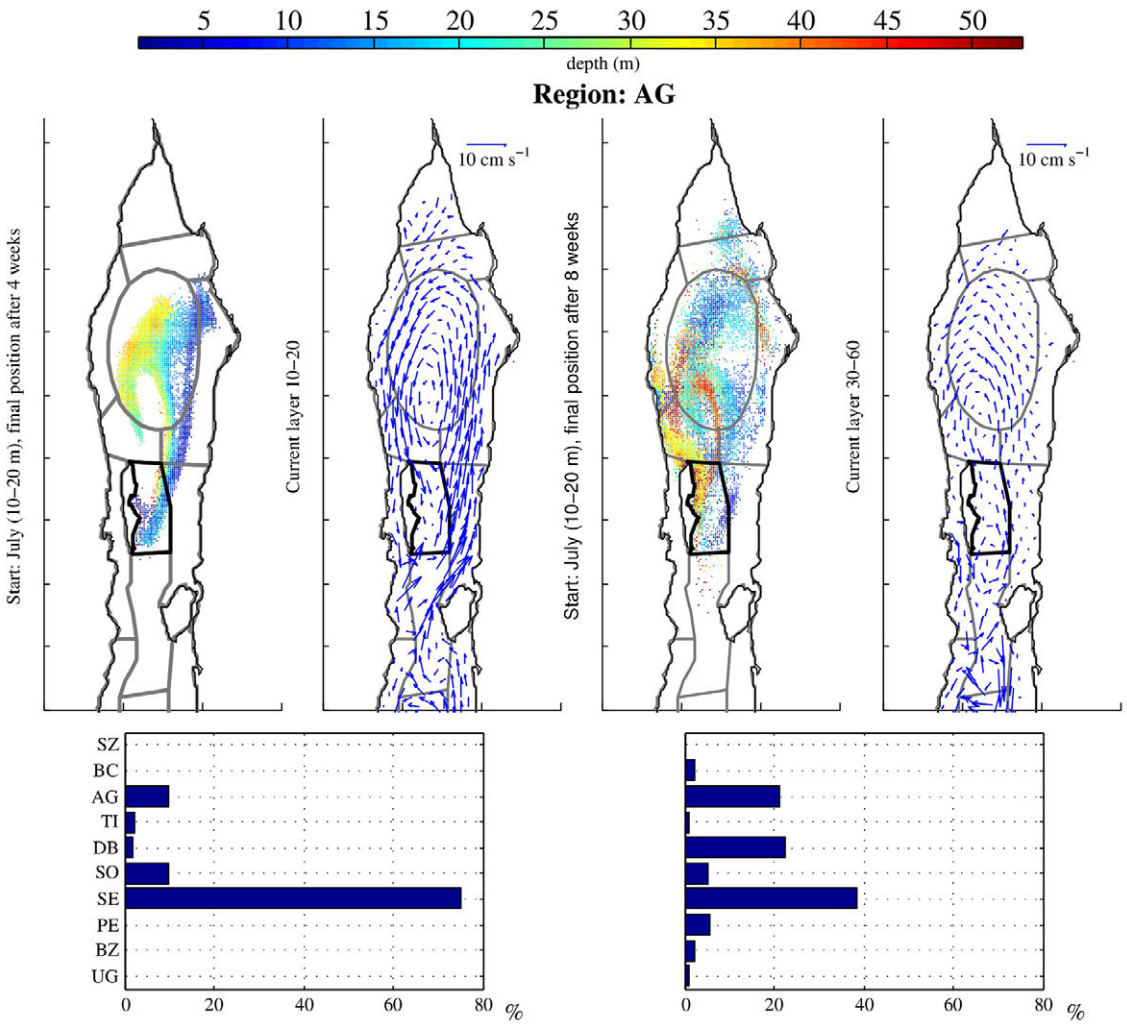

Fig. 11. – Map of final position of particles released in the east of the Ángel de la Guarda island's second layer, in the fourth and eighth week after the release of particles. The release area is shown in black and the other areas in grey polygon. The colour bar represents the depth at which each particle is located. The histogram shows the percentage of particles retained or transferred to other regions. Current maps correspond to the layer in which the percentage of particles retained is concentrated, in the fourth and eighth week after particle release.

Maximum catchment matrix

Figure 13A shows the maximum catchment matrix connectivity with its associated depth destination matrix (Fig. 13B) corresponding to the layer in which the particles were released after eight weeks. For example, more than 70% of the particles released in the Buffer Zone at 0-10 m depth ended up in the Upper Gulf area (number 1, Fig. 13A) at depths of 10-20 m (Fig. 13B).

Based on this matrix, most particles released in the various regions of the NGC were carried to the Seasonal Eddy (number 4; Fig. 13A), so the Seasonal Eddy is regarded as an area of high catchment where particles are trapped (Table 2). Other regions also displayed significant particle exchanges with other areas. This is the case of Ángel de la Guarda and Delfín Basin: the highest percentage of particles found below 200 m in the Sills Zone came from these regions (Fig. 13B).

In contrast, the particles released in the Seasonal Eddy were carried to Delfín Basin (Fig. 13A). This transport pattern is due to the fact that the centre of the eddy is located between the Seasonal Eddy and Delfín Basin areas during July and August (Fig. 2), causing the particles to be carried towards Delfín Basin.

Connectivity paths

Based on the transport of particles in relation to the predominant currents during the summer, we developed by visual inspection a diagram or sketches of surface connectivity (upper part of the water column) (Fig. 14A) and another for deep connectivity (lower part of the water column) (Fig. 14B). Both diagrams show the dominant paths of the particles due to the NGC circulation.

The main pathways in the upper layers were as follows: (1) The continental coastal current, which originated in the southern Gulf of California and passed through the Midriff Archipelago region, where its intensity increased, carried most of the particles in that area, i.e. those in the Sills Zone, Ángel de la Guarda and Tiburón Island. This current met the cyclonic eddy (2) in the interior of the gulf, and the particles carried by the continental coastal current (Sonora) were

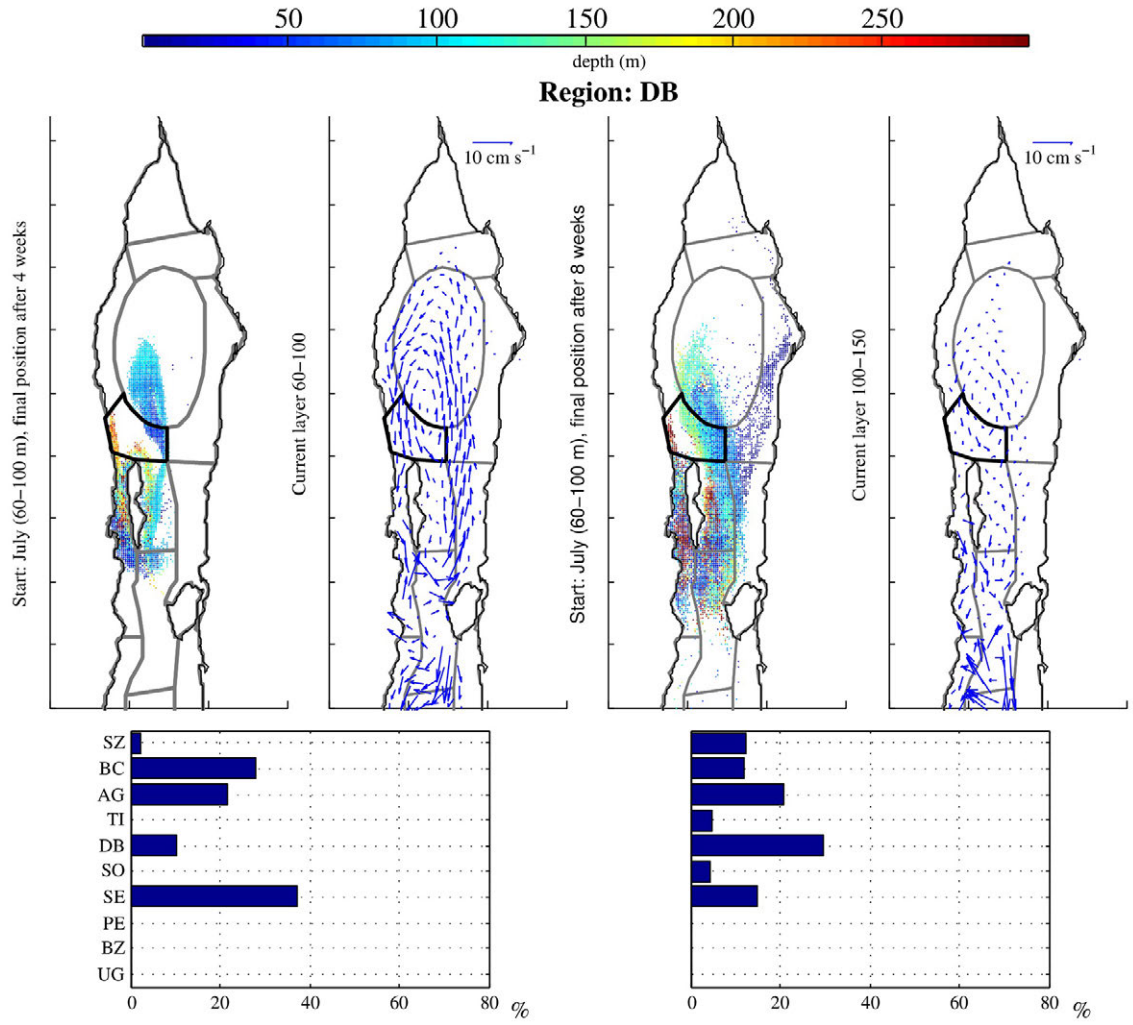

Fig. 12. – Map of final positions of particles released in the Delfín Basin's fifth layer, in the fourth and eighth week after the release of particles. The release area is shown in black and the other areas in grey polygon. The colour bar represents the depth at which each particle is located. The histogram shows the percentage of particles retained or transferred to other regions. Current maps correspond to the layer in which the percentage of particles retained is concentrated, in the fourth and eighth week after particle release.

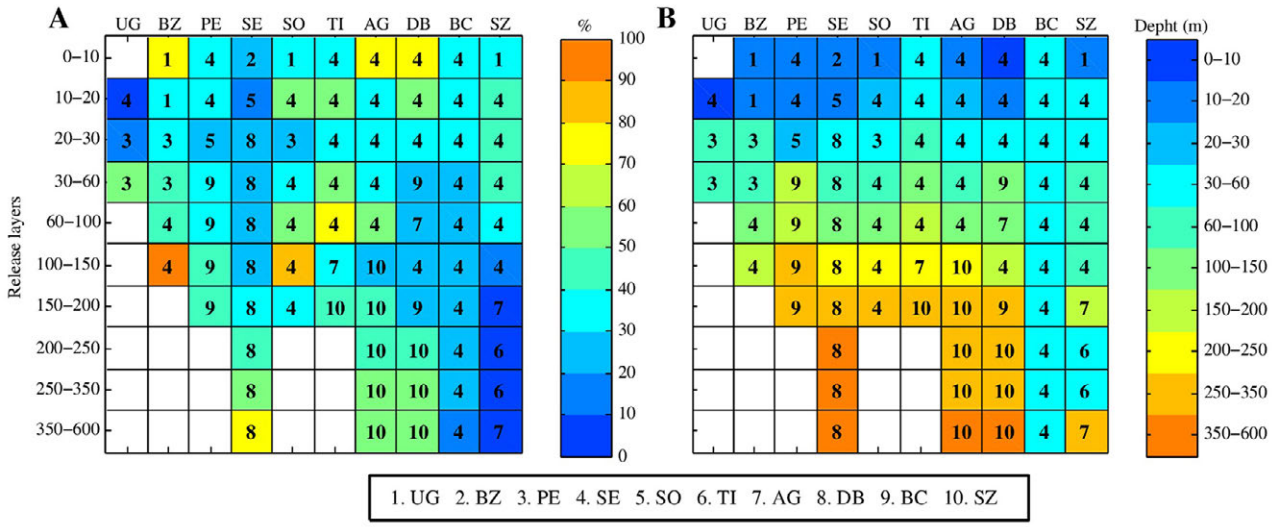

Fig. 13. – A, maximum catchment matrix, showing the cells for each released area and layer that had the highest percentage of particles, after eight weeks, excluding the diagonal elements of the connectivity matrices and indicated with digits; see box located at the bottom of the figure. B, final average depth matrix associated with the maximum catchment matrix.

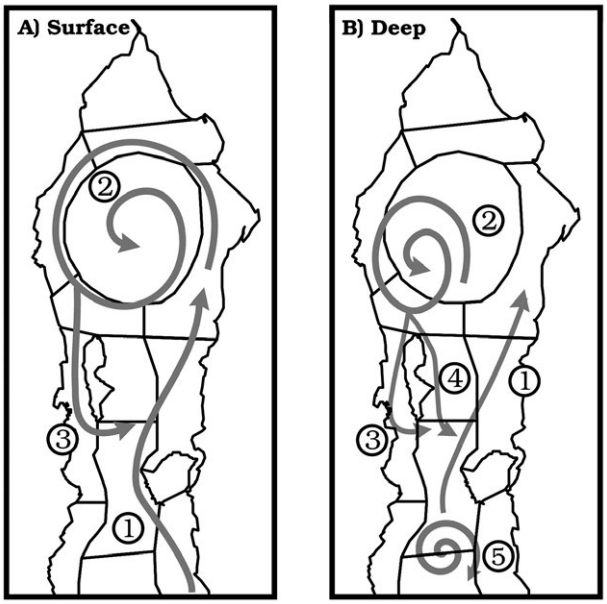

Fig. 14. – A, map of the northern Gulf of California with the preferred particle surface routes, related to the different structures of the movement: 1, coastal mainland current; 2, cyclonic eddy; and 3, Ballenas Channel current. B, map of the northern Gulf of California with the preferred deep routes of the particles, related to the different structures of the movement: 1, current coastal mainland; 2, cyclonic eddy; 3, Ballenas Channel current; 4, Current caused by the presence of Ángel de La Guarda island; and 5, anticyclonic eddy.

then carried by this eddy, whereby the particles from adjacent regions (Buffer Zone, Peninsular Eddies and Delfín Basin) were carried towards the centre of the Seasonal Eddy. However, the presence of Ángel de la Guarda island controlled a current that carried the particles from the Ballenas-Salsipuedes Channel to the southern gulf. As this current flowed away from the island, it met the continental coastal current (1), and the particles were carried to the northern gulf again.

The main pathways in the deep areas are shown in Figure 14B. Three of these pathways are similar to those observed in the upper layers (Fig. 14B). These include a current caused by a bifurcation of flow associated with the Seasonal Eddy and the location of Archangel Island (4). This current carried particles from the Seasonal Eddy, Delfín Basin and other locations affected by the reversible gyre to the Midriff Archipelago region. This current then joined the continental coastal current, which weakened with depth (see Fig. 2). Finally, a gyre (5) located south of Tiburón Island, in the San Pedro Mártir Basin, was observed by Marinone (2003) and Mateos et al. (2006). This eddy carried particles towards the interior of the gulf and the southern gulf.

CONCLUSIONS

A three-dimensional connectivity description of the northern Gulf of California has been presented. The final position of particle trajectories was calculated from the currents obtained by the HAMSOM baroclinic numerical model. From typical connectivity matrices in which the destination of particles from the released areas are shown, we constructed (i) a retention matrix that quantifies how many particles remain in each region and within the water column and (ii) a maximum catchment matrix that identifies the regions that capture most particles from the other regions. These matrices enabled us to identify significant patterns, such as areas where the greatest retention, dispersion and particle trapping occurred both horizontally and in the different layers of the water column. The specific cases identified with these matrices are presented in relation to the circulation and dispersion of particles for the summer season.

The Upper Gulf and the Seasonal Eddy were the locations retaining the largest percentages of particles along the water column, while north of Tiburón Island, the northern coast of Sonora, the Buffer Zone and the Peninsular Eddies region showed the smallest retention of particles due to the presence of a strong up-gulf coastal current.

The various patterns obtained from the retention matrix indicate that the behaviour of the particles released during the summer in the northern Gulf of California was controlled by the typical summer circulation patterns. Primary control was exerted by the interaction between the coastal continental current and the seasonal cyclonic eddy.

ACKNOWLEDGEMENTS

This research is a product of the MSc thesis of the first author, for which she was supported by a CONACyT scholarship. Financial support came from the CICESE regular budget and CONACyT Grant No. 44055. We want to thank two anonymous reviewers for their very useful suggestions to improve this article.

REFERENCES

Arvizu-Martinez J. 1987. Fisheries activities in the Gulf of California, Mexico. CalCOFI Report, 28: 32-36.

Beier E., Ripa P. 1999. Seasonal Gyres in the Northern Gulf of California. J. Phys. Oceanogr. 29: 302-311. http://dx.doi.org/10.1175/1520-0485(1999)029<0305:SGITNG>2.0.CO;2

Calderón-Aguilera L.E., Marinone S.G., Aragón-Noriega A.E. 2003. Influence of oceanographic processes on the early life stages of the blue shrimp (Litopenaeus stylirostris) in the upper Gulf of California. J. Mar. Syst. 39: 117-128. http://dx.doi.org/10.1016/S0924-7963(02)00265-8

Cudney-Bueno R., Lavín M.F., Marinone S.G., et al. 2009. Rapid Effects of Marine Reserves via Larval Dispersal. PLoS ONE 4: e4140. http://dx.doi.org/10.1371/journal.pone.0004140

Carrillo L., Lavín M.F., Palacios Hernández E. 2002. Seasonal evolution of the geostrophic circulation in the northern Gulf of California. Estuar. Coast. Shelf S. 54: 157-173. http://dx.doi.org/10.1006/ecss.2001.0845

Gutiérrez O.Q. 2002. Circulacion Lagrangeana en el Golfo de California. M.Sc. thesis. Centro de Investigación Científica y de Educación Superior de Ensenada, B.C., México. 70 pp.

Gutiérrez O.Q., Marinone S.G., Parés Sierra A. 2004. Lagrangian surface circulation in the Gulf of California from a 3D numerical model. Deep-Sea Res. Part II. 51: 659-672. http://dx.doi.org/10.1016/j.dsr2.2004.05.016

Lavín M.F., Marinone S.G. 2003. An overview of the physical oceanography of the Gulf of California. In: Velasco Fuentes O.U., Sheinbaum J., Ochoa J. (eds), Nonlinear processes in geophysical fluid dynamics. Kluwer Academic Publishers, pp. 173-204.

http://dx.doi.org/10.1007/978-94-010-0074-1_11
Lavín M.F., Durazo R., Palacios E., et al. 1997. Lagrangian observations of the circulation in the northern Gulf of California. J. Phys. Oceanogr. 27: 2298-2305. http://dx.doi.org/10.1175/1520-0485(1997)027<2298:LOOTCI>2.0.CO;2
Ledesma-Vázquez J., Carreño A.L. 2010. Origin, Age, and Geological Evolution of the Gulf of California. In: Brusca R.C. (ed.), The Gulf Of California: Biodiversity and Conservation. The University of Arizona Press, pp. 7-23.
Lluch-Cota S.E., Aragón-Noriega E.A., Arreguín-Sánchez F., et al. 2007. The Gulf of California: Review of ecosystem status and sustainability challenges. Prog. Oceanogr. 73: 1-26. http://dx.doi.org/10.1016/j.pocean.2007.01.013
López M., Candela J., Argote M.L. 2006. Why does the Ballenas Channel have the coldest SST in the Gulf of California? Geophys. Res. Lett. 33: 1-5. http://dx.doi.org/10.1029/2006GL025908
López M., Candela J., García J. 2008. Two overflows in the Northern Gulf of California. J. Geophys. Res. 113: 1-12. http://dx.doi.org/10.1029/2007JC004575
Marinone S.G. 2003. A three-dimensional model of the mean and seasonal circulation of the Gulf of California. J. Geophys. Res. 108: 1-27. http://dx.doi.org/10.1029/2002JC001720
Marinone S.G. 2006. A numerical simulation of the two-and three-dimensional Lagrangian circulation in the northern Gulf of California. Estuar. Coast. Shelf S. 68: 93-100. http://dx.doi.org/10.1016/j.ecss.2006.01.012
Marinone S.G. 2008. On the three-dimensional numerical modeling of the deep circulation around Ángel de la Guarda Island in the Gulf of California. Estuar. Coast. Shelf S. 80: 430-434. http://dx.doi.org/10.1016/j.ecss.2008.09.002
Marinone S.G. 2012. Seasonal surface connectivity in the Gulf of California. Estuar. Coast. Shelf S. 100: 133-141. http://dx.doi.org/10.1016/j.ecss.2012.01.003
Marinone S.G., Lavín M.F. 2005. Tidal Current Ellipses in a 3D Baroclinic Numerical Model of the Gulf of California, Estuar. Coast. Shelf S. 31: 357-368.
Marinone S.G., Ulloa M.J., Parés Sierra A., et al. 2008. Connectivity in the northern Gulf of California from particle tracking in a three-dimensional numerical model. J. Mar. Sys. 71: 149-158. http://dx.doi.org/10.1016/j.jmarsys.2007.06.005
Marinone S.G., Lavín M.F., Parés Sierra A. 2011. A quantitative characterization of the seasonal Lagrangian circulation of the Gulf of California from a three dimensional numerical model. Cont. Shelf Res. 31: 1420-1426. http://dx.doi.org/10.1016/j.csr.2011.05.014
Mateos E., Marinone S.G., Lavín M.F. 2006. Role of tides and mixing in the formation of an anticyclonic gyre in San Pedro Mártir Basin, Gulf of California. Deep-Sea Res Part II. 53: 60-76. http://dx.doi.org/10.1016/j.dsr2.2005.07.010
Munguia-Vega A., Jackson A., Marinone S.G., et al. 2014. Asymmetric connectivity of spawning aggregations of a commercially important marine fish using a multidisciplinary approach. PeerJ. 2: e511. http://dx.doi.org/10.7717/peerj.511
Peguero-Icaza M., Sánchez Velasco L., Lavín M.F., et al. 2011. Seasonal changes in connectivity routes among larval fish assemblages in a semi-enclosed sea (Gulf of California). J. Plankton Res. 33: 517-533. http://dx.doi.org/10.1093/plankt/fbq107
Proehl J.A., Lynch D.R., McGillicuddy D.J., et al. 2005. Modeling turbulent dispersion on the North Flank of Georges Bank using Lagrangian particle methods. Cont. Shelf Res. 25: 875-900. http://dx.doi.org/10.1016/j.csr.2004.09.022
Sánchez Velasco L., Lavín M.F., Jiménez Rosenberg S.P.A., et al. 2012. Larval fish habitats and hydrography in the Biosphere Reserve of the Upper Gulf of California (June 2008). Cont. Shelf Res. 33: 89-99. http://dx.doi.org/10.1016/j.csr.2011.11.009
Santiago-García M.W., Marinone S.G., Velasco-Fuentes O.U. 2014. Three-dimensional connectivity in the Gulf of California based on a numerical model. Prog. Oceanogr. 123: 64-73. http://dx.doi.org/10.1016/j.pocean.2014.02.002
Soria G., Torre-Cosio J., Munguia-Vega A., et al. 2013. Dynamic connectivity patterns from an insular marine protected area in the Gulf of California. J. Mar. Sys. 129: 248-258. http://dx.doi.org/10.1016/j.jmarsys.2013.06.012
Velasco Fuentes O.U., Marinone S.G. 1999. A numerical study of the Lagrangian circulation in the Gulf of California. J. Mar. Sys. 22: 1-12. http://dx.doi.org/10.1016/S0924-7963(98)00097-9
Visser A.W. 1997. Using random walk models to simulate the vertical distribution of particles in a turbulent water column. Mar. Ecol. Prog. Ser. 158: 275-281. http://dx.doi.org/10.3354/meps158275